

Structure Development and Property Changes in High Density Polyethylene During Pan-Milling

H. HUANG*

Polymer Research Institute, Sichuan University, Chengdu 610065, China

Received 18 August 1999; accepted 15 March 2000

ABSTRACT: A new self-designed mechanochemical reactor, inlaid pan-mill, was used in studying high density polyethylene (HDPE). The effects of pan-milling stress on the structure and properties of HDPE were investigated. Gel permeation chromatography, melt indexer, Fourier transformed infrared spectroscopy, electron spectroscopy for chemical analysis, differential scanning calorimetry, X-ray diffraction, capillary rheometer, and Instron material testing system were used to characterize the structures and evaluate the properties of HDPE. The results showed that mechanochemical degradation of HDPE occurred under the stress fields of pan-mill, the molecular weight of HDPE was reduced, and HDPE with higher initial molecular weights were easier to degrade under the stress fields. Oxygen-containing groups such as COOH, C=O, and C—O were introduced to HDPE chains as a result of degradation during milling. Crystallinity of HDPE first decreased slightly followed by gradual increases with increasing milling times; monoclinic crystals appeared after four cycles of milling and increased markedly with increasing milling times. Pressure oscillation in capillary flow occurred at significantly higher shear stress and shear rate for milled HDPE than unmilled HDPE. After milling, mechanical properties were improved. © 2000 John Wiley & Sons, Inc. *J Appl Polym Sci* 78: 2016–2024, 2000

Key words: high density polyethylene; pan-milling; structure; properties

INTRODUCTION

Stress reactions of polymers, a field often called mechanochemistry, are the object of intensive research.¹ When handling high molecular weight polymers, stress reactions must be considered. Application of stress may result in changes in supermolecular structure and the rupture of chemical bonds. Molecular topology is changed, i.e., molecular weight and its distribution, and branching and crosslinking. Stress reactions may

be observed for amorphous polymer chains in dilute solutions and in polymer melts; they may also be observed for semicrystalline or amorphous polymers in the solid state. The modes of stress reaction in the solid state may be classified into four categories: comminution (grinding, milling, and crushing); machining (drilling, cutting, and slicing); stretching; and other means (fatigue, tear, and wear tests).

Frictional wear in relation to milling of solid polymers has been studied by Nash et al.² Graham³ has reported on shock-induced electrical activity in polymeric solids, especially in poly(pyromellitimide), and proposed a model for mechanically induced bond scission based on shock-induction of polarization and conduction. The mechanochemical effects of moisture on epoxy resins has been demonstrated by Fourier trans-

* Permanent address: School of Chemistry and Chemical Engineering, Shanghai Jiao Tong University, Shanghai 200240, China (ncliu@mail.sjtu.edu.cn).

Contract grant sponsors: National Science Foundation of China and State Education Commission of China.

Journal of Applied Polymer Science, Vol. 78, 2016–2024 (2000)
© 2000 John Wiley & Sons, Inc.

form infrared (FTIR) spectroscopy.⁴ A mechanism has been proposed for interatomic (intermolecular) bond breakage in polymer fibers.⁵ A range of milling techniques has been applied by Romanian researchers^{6–9} in synthesizing different polymers and copolymers. Polyethylene (PE) was produced mechanochemically by milling of alumina powder at room temperature in the presence of ethylene monomer.¹⁰ Xu and Guo¹¹ produced low molecular weight polyvinyl chloride (PVC) by degrading PVC in ball mills and used the degraded PVC to plasticize high molecular weight PVC.

One characteristic of stress reactions in the solid state is that mechanochemical degradation mainly processes at the broken surfaces of particles during pulverizing.¹² Therefore, pulverizing materials effectively is an essential factor for mechanochemical degradation. Pulverizing of brittle materials may be attained easily by using traditional equipment such as a ball-mill; however, it is quite difficult for ductile materials. Stress reaction of PE at room temperature is rarely studied because of equipment limitation. There are only a few articles about the detection of macroradicals formed during ball-milling of PE powder at liquid nitrogen temperature by the electron-spin resonance technique.^{13,14}

Xu and Wang¹⁵ designed an innovative piece of equipment, an inlaid pan-mill, on the basis of a traditional Chinese stone-mill. One of the distinct features of the pan-mill is that it can exert extremely strong shear forces on materials in-between because of its inlaid structure. In addition, the general moving path of materials in the pan-mill is spiral which increases residence time.^{16–18} Experimental results demonstrated that this innovative equipment is not only superior to existing equipment in pulverizing brittle materials such as polystyrene (PS), but is also effective in pulverizing ductile materials such as high density polyethylene (HDPE).^{16–18} Wang et al.¹⁹ have studied the interactions between PS and TiO₂ during the pan-milling process.

In this report, pan-mill equipment was chosen as a good candidate for the mechanical processing of ductile HDPE; the effects of pan-milling stress on the structure and properties of HDPE were studied.

EXPERIMENTAL

Materials

Unless otherwise stated, the HDPE used was HDPE6098 with a melt index of 0.1 dg/min and a

density of 0.948 g/cm³, supplied by Qilu Petrochemical Company (Shandong, China).

Pan-Milling

An inlaid pan-mill-type mechanochemical reactor¹⁵ with water-cooling and a rotating speed of 25 rpm, was used. HDPE was milled for different times (cycles). The process from the beginning of feeding to the end of material discharge was considered as one cycle.

Characterization

Molecular weight was determined by using a PL-GPC-210 gel permeation chromatography. Orthodichlorobenzene was used with a flow rate of 1.0 mL/min at 160°C. PS was used as reference.

The melt index was measured at 190°C with 5-kg load unless otherwise stated according to ASTM D1238 E.

HDPE samples were compression molded into thin films with a thickness of approximately 100 μm for FTIR and electron spectroscopy for chemical analysis (ESCA). A Nicolet 170X FTIR spectrometer and a Kratos XSAM 80 electron spectrometer with an Al K_α irradiation source were used. Peak separation for C_{1s} spectra was performed automatically according to Gauss distribution.

Wide angle X-ray diffractograms were recorded using a D/Max IIA diffractometer with CuK_α radiation incident perpendicular to the sample plane and draw axis.

Property Testing

Unmilled and milled HDPE were plasticated in a Brabender W50H mixer at 180°C and 40 rpm for 10 min, followed by compression molding at 190°C. Tensile tests were performed on an Instron 4302 Materials Testing System at a rate of 50 mm/min according to GB1040-79. Rheological measurements were taken on a Goffert 2002 capillary rheometer; Bagley correction was not done.

RESULTS AND DISCUSSION

Mechanochemical Degradation

Molecular weights of unmilled and milled HDPE are shown in Figure 1. Molecular weight decreased gradually with increasing times of mill-

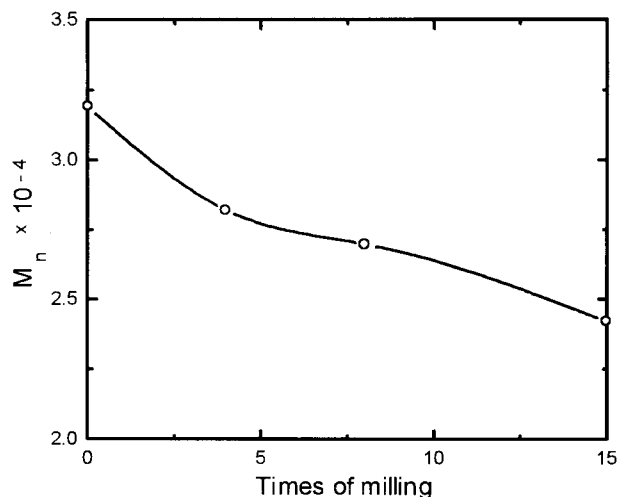


Figure 1 Effect of times of milling on the molecular weight of HDPE.

ing, confirming the degradation of HDPE during pan-milling.

Initial molecular weight is an important factor influencing the mechanochemical degradation of polymers. Figure 2 shows the influence of initial melt index on the mechanochemical degradation of HDPE. Melt indices for all three samples increased with increasing milling times. Because melt index is inversely proportional to molecular weight, therefore, the extent of HDPE degradation increased with increasing milling times. Nevertheless, the extent of degradation was different for HDPE with different initial melt index, which can be better seen in Table I. For HDPE with higher initial molecular weights, HDPE7000F and HDPE6098, melt index increased to approximately 60% after milling for 15 times, whereas an increase in melt index of HDPE7006A (with lower initial molecular weight) was less than 10%. These indicate that HDPE with higher initial molecular weight is easier to degrade under stress field.

Effect of Pan-Milling on HDPE Structures

Mechanochemical degradation is often accompanied by the introduction of polar groups onto polymer chains. Figure 3 shows the infrared spectra of HDPE before and after milling. The absorbance at 1194 cm^{-1} characteristic of C—O stretching and at 1743 cm^{-1} characteristic of C=O groups clearly indicates the presence of oxygen-containing groups in the milled HDPE. Furthermore, the intensities of those peaks increased with increas-

ing milling times. This is further supported by ESCA results as shown in Figure 4 and Table II. The O/C ratio of HDPE increased from approximately 5.0 to 8.3% after milling for 10 times. After peak separation of C_{1s} , C(=O)—O, C=O, and C—O groups were clearly seen in the milled HDPE. The introduction of oxygen-containing groups is due to the reaction of oxygen in air and HDPE macroradicals resulted from chain scission under strong pan-milling stress.

Figure 5 shows the differential scanning calorimetry (DSC) curves of milled and unmilled HDPE. There is no significant change in the position and intensity of the melting peak. These are better seen in Table III. Melting points for HDPE samples milled for different times are in between 130 and 132°C . Crystallinity of HDPE first decreased with increasing milling times, but increased with increasing milling times after two cycles of milling. Nevertheless, the change in crystallinity was only about 4%, which is rather small considering the high stress applied to the polymer in the pan-mill. Could there be a crystal form transformation occurring during milling? If that was the case, the high stress in pan-mill resulting in crystal form transformation might not cause much change in crystallinity as evidenced by DSC analysis.

Crystal forms of PE include stable orthorhombic [$P_{\text{nam}}(D_{2h}^{16})$] with cell dimensions of $a = 7.417\text{ \AA}$, $b = 4.945\text{ \AA}$, $c = 2.547\text{ \AA}$, metastable monoclinic [$C2/m(C_{2h}^3)$] with cell dimensions of $a = 8.09\text{ \AA}$, $b = 2.53\text{ \AA}$, $c = 4.79\text{ \AA}$, $\beta = 107.9^\circ$ and high pressure orthohexagonal. Both orthorhombic and monoclinic phases have planar zigzag structures. Orthorhombic forms have two distinct diffraction

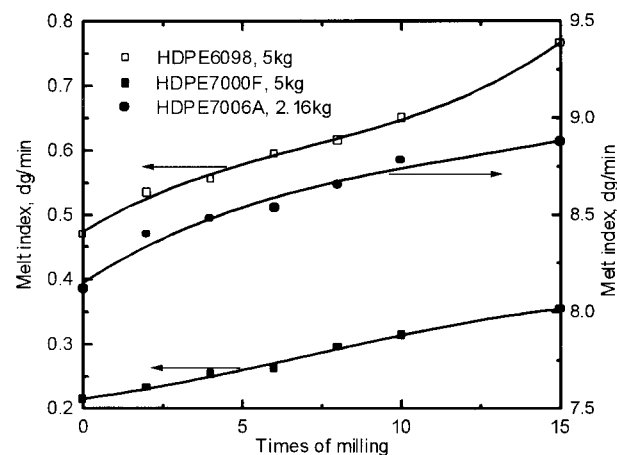


Figure 2 Melt indices of various milled HDPE.

Table I Effect of Initial Molecular Weight on MI on HDPE

Sample	HDPE6098	HDPE7000F	HDPE7006A
Initial MI of HDPE (MI_0 , dg/min)	0.47	0.21	8.12 (2.16 kg)
MI of HDPE milled for 15 times (MI_{15} , dg/min)	0.77	0.35	8.88 (2.16 kg)
$(MI_{15} - MI_0)/MI_0$ (%)	60	63	9.3

peaks at $2\theta = 21.4^\circ$ (110, $d_{110} = 4.1\text{\AA}$) and $2\theta = 23.65^\circ$ (200, $d_{200} = 3.715\text{\AA}$), whereas monoclinic forms have a strong diffraction peak at $2\theta = 19.5^\circ$ (001, $d_{001} = 4.55\text{\AA}$) and two weak peaks at $2\theta = 14.1^\circ$ (110, $d_{110} = 6.276\text{\AA}$) and $2\theta = 17.1^\circ$ (040, $d_{040} = 5.180\text{\AA}$). Because the amorphous phase has a wide diffraction band at $2\theta = 19.5^\circ$ ($d = 4.55\text{\AA}$) which is overlapping with the monoclinic phase, therefore, diffractions at $2\theta = 19.5^\circ$ must be used together with the other two diffraction peaks to confirm the presence of monoclinic crystals.

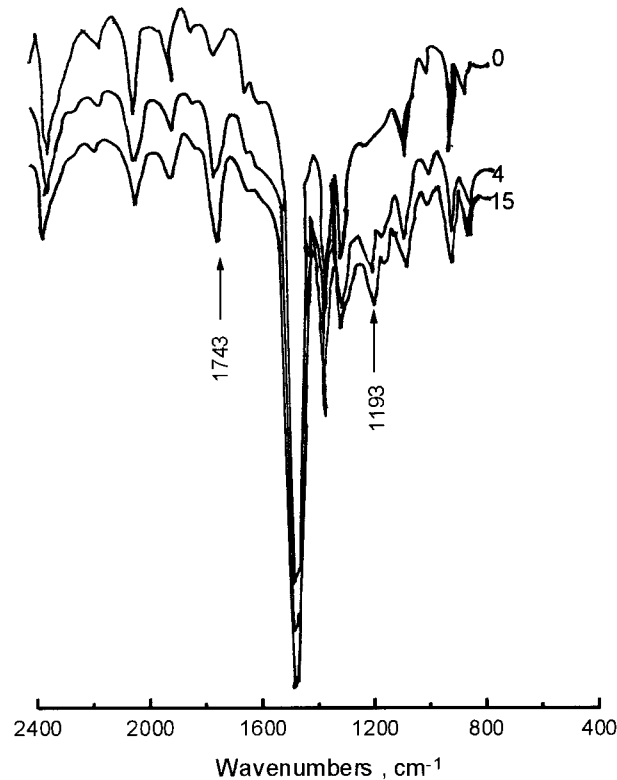
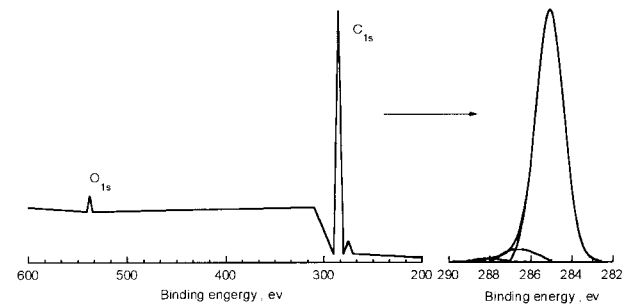
Figure 6 shows the X-ray diffraction curves of milled and unmilled HDPE. At milling times of four cycles, there appeared clearly the characteristic diffraction peaks of monoclinic crystals. The

intensity of the peaks became stronger at milling times of 15 cycles. Therefore, it may be concluded that monoclinic crystal phases were formed during pan-milling.

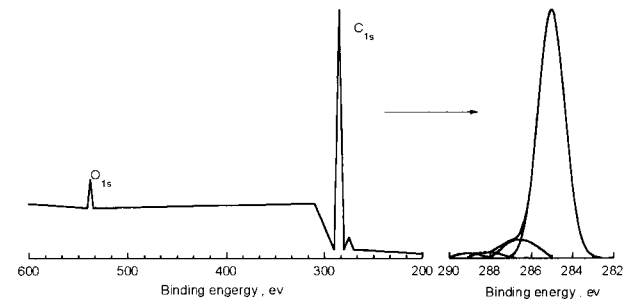
Crystallinity may be calculated after peak separation by Gauss function by using the following equation:

$$X_c = \frac{I_c}{I_c + KI_a} \times 100\%$$

where X_c is crystallinity, I_c and I_a are peak intensities for crystalline and amorphous peaks respectively, K is constant (0.75 for PE). The calculated results are plotted in Figure 7. Crystallinity ini-

**Figure 3** FTIR spectra of milled and unmilled HDPE (numbers indicate times of milling).

(a) unmilled HDPE



(b) HDPE milled 10 times

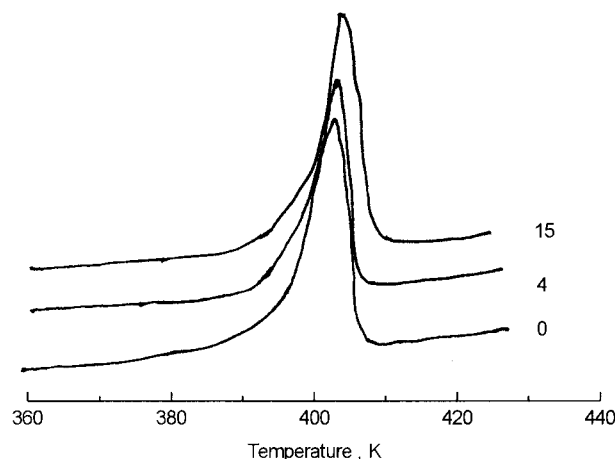
Figure 4 ESCA of unmilled (a) and milled (b) HDPE.

Table II ESCA Results of Milled and Unmilled HDPE

	Unmilled HDPE	HDPE Milled 10 Times
$\text{C}-\text{H}_2$		
Binding energy (ev)	285.0	285.0
FWHM (ev)	1.5	1.5
Area (%)	92.0	88.0
$\text{C}-\text{O}$		
Binding energy (ev)	286.6	286.6
FWHM (ev)	1.5	1.5
Area (%)	5.5	7.1
$\text{C}=\text{O}$		
Binding energy (ev)	287.9	287.9
FWHM (ev)	1.5	1.5
Area (%)	0.8	1.3
$\text{C}(=\text{O})\text{O}$		
Binding energy (ev)	289.1	289.1
FWHM (ev)	1.5	1.5
Area (%)	0.1	1.7
O/C		
Atomic ratio (%)	5.0	8.3

tially decreased with increasing times of milling, which is followed by gradual increases. This is in good agreement with the DSC analysis results shown above.

With the same peak separation method by Gauss function, the proportions of monoclinic (R_{mc}) and orthorhombic (R_{or}) phases in the crystal part of milled and unmilled HDPE are similarly calculated and plotted in Figure 8. With increasing times of milling, the proportion of the monoclinic phase increased markedly while the propor-

**Figure 5** DSC curves of milled and unmilled HDPE (numbers indicate times of milling).**Table III DSC Analysis Results of Milled and Unmilled HDPE**

Milling Times (Cycles)	Melting Point (°C)	Enthalpy (J/g)	Crystallinity (%)
0	130.2	153	53.6
2	130.2	145	50.9
4	130.2	148	51.9
6	132.0	149	52.0
8	131.3	155	54.4
10	131.0	157	54.9
15	130.3	157	55.0

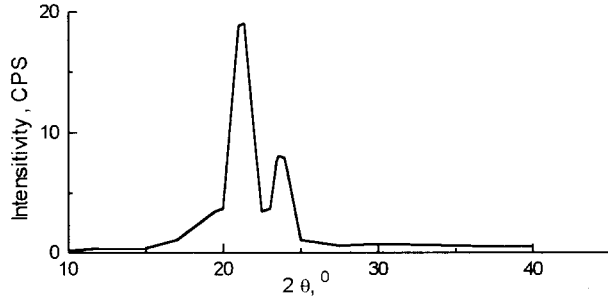
tion of orthorhombic phase decreased greatly. After 15 times of milling, the proportion of the monoclinic phase increased from 0% to approximately 40% whereas the proportion of the orthorhombic phase decreased from 100% to approximately 60%.

Under pan-milling stress, a part of HDPE crystals may be destroyed into amorphous phase, resulting in the initial decrease of crystallinity at low milling times. Shear stress may also result in crystal form transformation (orthorhombic form to monoclinic form) as reported in the literature.^{20–24} However, this could not explain the experimental results that the total crystallinity of HDPE at high milling times was even higher than the initial crystallinity of HDPE without milling. The reason for the increase of crystallinity at high milling times may be explained by the following proposed mechanism²⁵: in addition to the crystal form transformation from orthorhombic to monoclinic, a part of the short-range orderly structure in amorphous phase may be transformed into monoclinic crystal phase during pan-milling.

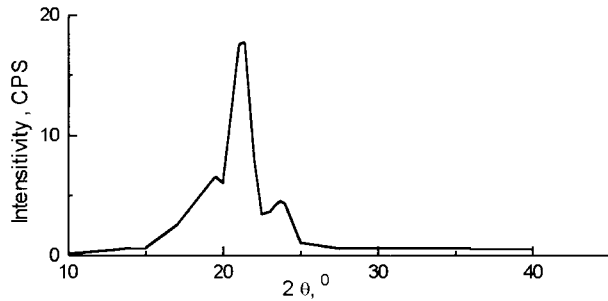
Effect of Pan-Milling on Rheological Properties of HDPE

It has been known that sharkskin roughness occurs for HDPE (indicated on flow curves by a change of slope in the steady flow region) when the shear stress surpasses the first critical value (σ_{c1}), and driving pressure and flow rate oscillate once the shear stress surpasses the upper critical value (σ_{c2}) while piston speed is in a certain range.

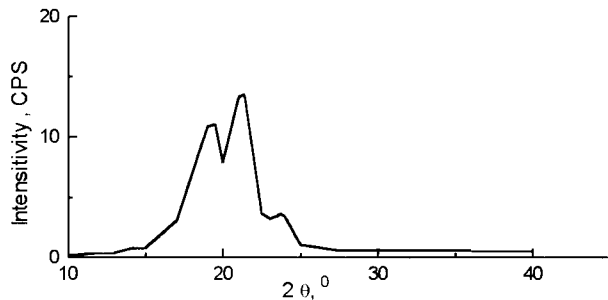
Figure 9 shows the apparent flow curve of unmilled and milled HDPE measured at 220°C using a die with a diameter of 1 mm and an L/D ratio of 10 (Bagley correction was not performed). There was no significant difference in the low



(a) Unmilled HDPE



(b) HDPE milled 4 times



(c) HDPE milled 15 times

Figure 6 X-ray diffraction curves of HDPE: unground (a), milled four times (b), and milled 15 times (c).

shear rate part of the flow curves of milled and unground HDPE. For HDPE milled for 15 times, pressure oscillating occurred at significantly higher shear stress and shear rate. Values of shear rate at which oscillating flow occurred, the first and upper critical shear stresses were calculated and are listed in Table IV. σ_{c1} was about the same at 0.11 MPa for both unground and milled HDPE. σ_{c2} was significantly higher for milled

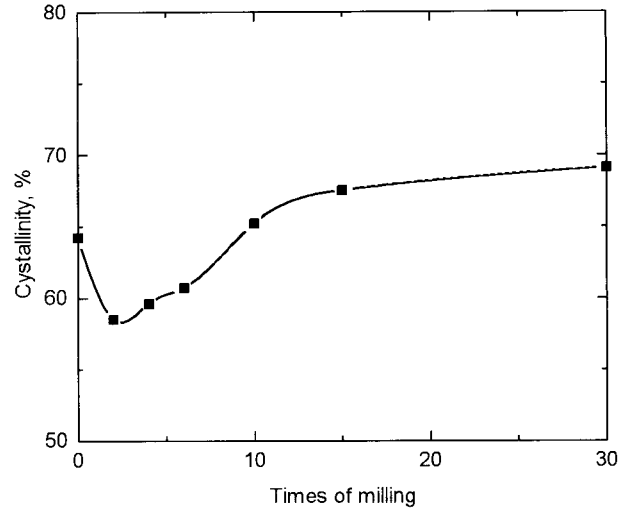


Figure 7 Crystallinity (X_c) of milled and unground HDPE measured by X-ray diffraction method.

HDPE than unground HDPE. Oscillating flow occurred at a shear rate of 460 s^{-1} for HDPE after milling for 15 times, which was about two times of that for unground HDPE.

The above oscillating phenomenon may be explained by the well-accepted slip-stick mechanism for flow instability. As the slip-stick mechanism explains, slip will occur above a critical shear stress because of lack of cohesion between melt fluid and capillary surface, and the possible rise of temperature resulting from slip and energy release will make the melt fluid stick again. Because of the slip-stick process, instability appears in flow curve. The critical shear stress increases

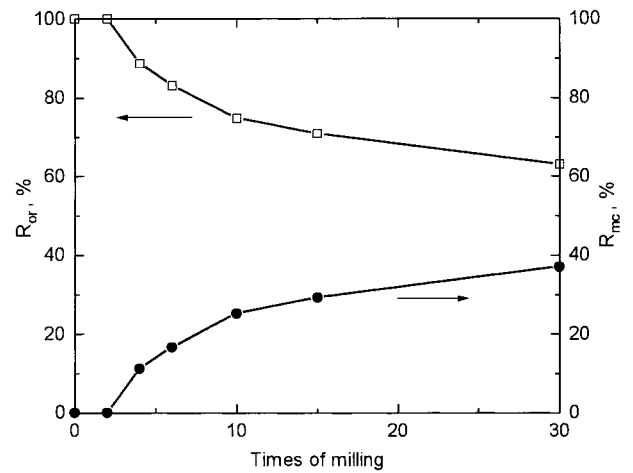


Figure 8 Proportion of orthorhombic (R_{or}) and monoclinic (R_{mc}) phases in milled and unground HDPE.

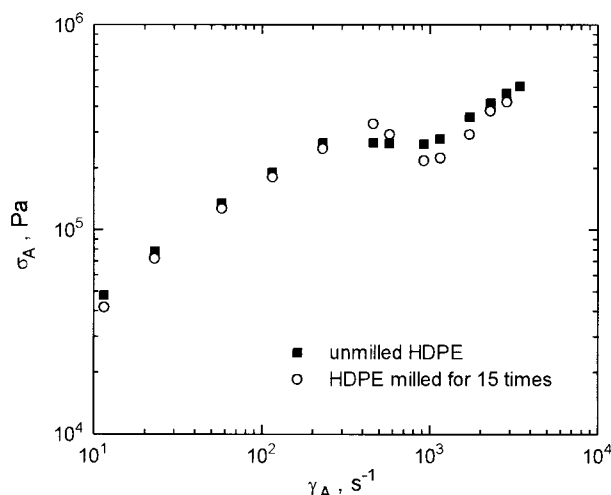


Figure 9 Apparent flow curve of HDPE ($D = 1.0$ mm, $L/D = 10$, $T = 220^\circ\text{C}$).

with the decrease of molecular weight. Because mechanochemical degradation of HDPE occurred under the stress fields of pan-mill, the molecular weight of HDPE was reduced and oxygen-containing groups were introduced to HDPE chains during milling which would increase the cohesion between melt fluid and capillary surface. Therefore, the upper critical shear stress (σ_{c2}) should be higher for milled HDPE than unmilled HDPE and the period of the oscillation should increase with increasing times of milling.

Apparent shear viscosities of milled and unmilled HDPE are plotted in Figure 10. When shear rate was in the low shear rate branch of the flow curve, apparent shear viscosity decreased with increasing times of milling during the steady flow, which is consistent with the result of the melt index. However, the difference of apparent shear viscosity between milled and unmilled HDPE became smaller at higher shear rates. This indicates that changes in molecular weight of HDPE caused by milling stress only have influ-

Table IV First Critical Shear Stress (σ_{c1}), Upper Critical Shear Stress (σ_{c2}), Apparent Shear Rate at Which Oscillating Flow Occurs ($\gamma_{A,O}$) of Milled and Unmilled HDPE

Times of Milling	0	8	15	30
σ_{c1} (MPa)	0.11	0.11	0.11	0.10
σ_{c2} (MPa)	0.26	0.28	0.33	0.29
$\gamma_{A,O}$ (s^{-1})	230	230	460	460

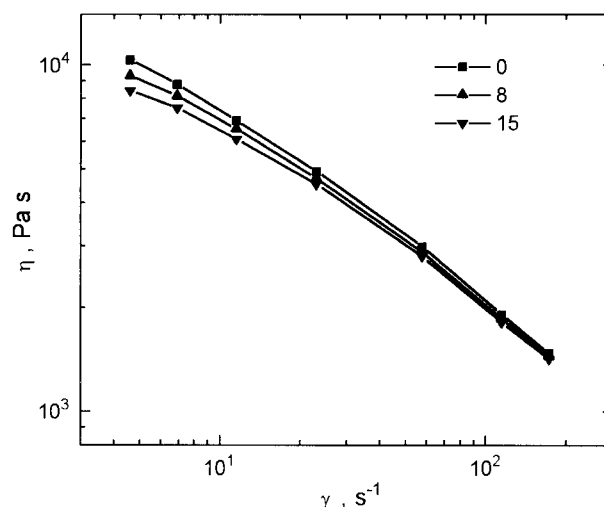


Figure 10 Apparent shear viscosity of milled and unmilled HDPE ($T = 190^\circ\text{C}$ and $L/D = 30$; numbers indicate times of milling).

ences on rheological behavior of HDPE during steady flow (before sharkskin roughness occurs), but have little influence after sharkskin roughness occurs.

Temperature dependency of apparent shear viscosity can be described by the Arrhenius equation:

$$\eta = Ae^{E/RT}$$

Figure 11 shows the relationship between apparent shear viscosity and the reciprocal of absolute temperature for unmilled HDPE and HDPE milled for 15 times. Flow activation energies (E) were calculated from the slopes of the linear portion of $\log\eta$ versus $1/T$ curves and are listed in Table V. At low shear rates, the flow activation energy of HDPE milled for 15 times is higher than that of unmilled HDPE, which may be a result of polar interactions between oxygen-containing groups introduced during milling. At shear rates higher than 20 s^{-1} , HDPE milled for 15 times had lower flow activation energy than unmilled HDPE; this may be explained by increases in the chain mobility of milled HDPE as a result of chain scission.

Effect of Pan-Milling on Mechanical Properties of HDPE

The tensile properties of milled and unmilled HDPE are shown in Table VI. After milling, ten-

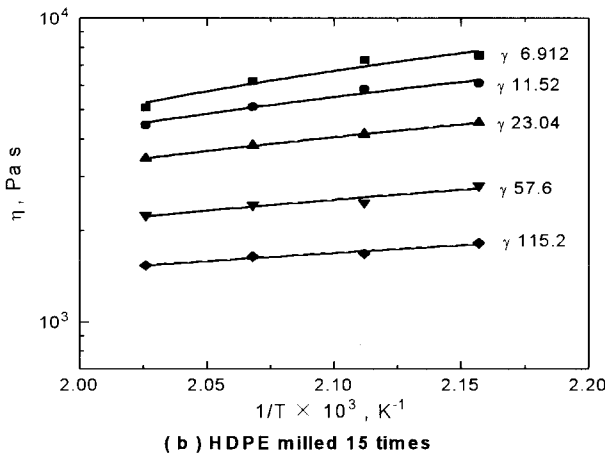
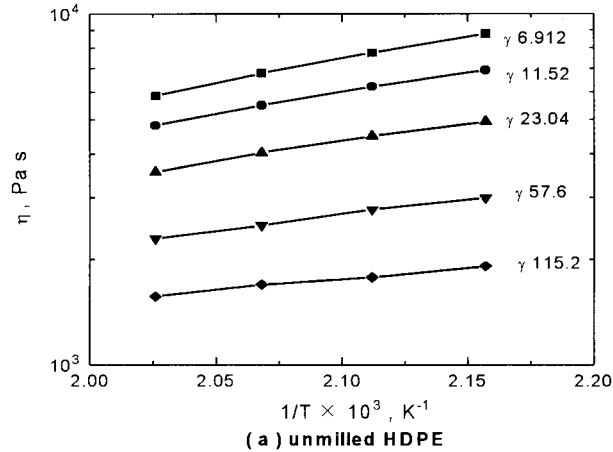


Figure 11 Relationship between $\log \eta$ and $1/T$ of (a) unmilled and (b) milled HDPE.

sile strength increases, the elongation at break of HDPE goes through a maximum whereas modulus goes in a reverse trend with increasing times of milling. HDPE with four times of milling has the best mechanical property in general. These could be due to structural changes of HDPE during pan-milling; however, the changes were not very significant.

Table V Flow Activation Energy of Unmilled HDPE (E_0) and HDPE Milled for 15 Times (E_{15})

γ (s^{-1})	E_0 (J/mol)	E_{15} (J/mol)
6.912	27.7	35.0
11.52	24.7	26.8
23.04	23.1	18.0
57.6	18.8	9.52
115.2	12.3	8.79

Table VI Mechanical Properties of Milled and Unmilled HDPE

Times of Milling (Cycles)	Tensile Strength (MPa)	Young's Modulus (MPa)	Elongation at Break (%)
0	17.29	1038	827.3
2	18.20	1003	865.2
4	19.41	1019	885.4
6	18.10	1131	836.9
8	18.34	1171	812.2
10	18.94	1194	784.9
15	19.03	1243	776.6

CONCLUSIONS

1. Mechanochemical degradation of HDPE occurred under the stress fields of pan-mill; the molecular weight of HDPE was reduced after milling. HDPE with higher initial molecular weights were easier to degrade under the stress fields.
2. Oxygen-containing groups such as COOH, C=O, and C—O were introduced to HDPE chains as a result of degradation during milling.
3. Crystallinity of HDPE first decreased slightly, followed by gradual increases with increasing milling times; monoclinic crystals appeared after four cycles of milling and increased markedly with increasing milling times.
4. The apparent shear viscosity of HDPE decreased with increasing times of milling. After milling, the flow activation energy decreased and thus sensitivity of viscosity to temperature was reduced. Pressure oscillation in capillary flow occurred at significantly higher shear stress and shear rate for milled HDPE than unmilled HDPE.
5. Mechanical properties of HDPE were improved after milling. HDPE with four times of milling had the best mechanical property in general.

REFERENCES

1. Porter, R. S.; Casale, A. *Polym Eng Sci* 1985, 25, 129.
2. Nash, R. J.; Jacobs, D. M.; Selig, R. F. *J Colloid Interface Sci* 1979, 70, 366.

3. Graham, R. A. *J Phys Chem* 1979, 83, 3048.
4. Graham, R. A.; Dodson, B. W. Sandia National Laboratories, Report SAND-80-1642, August, 1980.
5. Levy, R. L.; Fanter, D. L.; Summers, C. J. *J Appl Polym Sci* 1979, 24, 1043.
6. Vasiliu Oprea, C.; Popa, M. *Angew Makromol Chem* 1980, 90, 13.
7. Vasiliu Oprea, C.; Popa, M. *Angew Makromol Chem* 1980, 92, 1.
8. Vasiliu Oprea, C.; Weiner, F. *Angew Makromol Chem* 1982, 106, 207.
9. Vasiliu Oprea, C.; Negulianu, C.; Popa, M.; Weiner, F. *Bull Inst Polym Iasi* 1980, 26, 87.
10. Murakami, S.; Tabata, M.; Sohma, J. *J Appl Polym Sci* 1984, 29, 291.
11. Xu, X.; Guo, S. Y. *Polym Plast Technol Eng* 1995, 34, 621.
12. Baramboim, H. K. *Mechanochemistry of Polymers*; Chemical Industry Press: Moscow, 1978.
13. Casale, A.; Porter, R. S. *Polymer Stress Reactions*; Academic Press: New York, 1978; Vol. 2.
14. Vivatpanachart, S.; Nomura, H.; Miyahara, Y.; Kashiwabara, H.; Sakaguchi, M. *Polymer* 1981, 22, 132.
15. Xu, X.; Wang, Q. Chinese Pat. CN 2217463Y, 1995.
16. Xu, X.; Wang, Q.; Kong, X. A.; Zhang, X. D.; Huang, J. G. *Plast Rubber Compos Process Appl* 1996, 25, 152.
17. Xu, X.; Wang, Q. The Polymer Processing Society, European Meeting, Stuttgart, Germany, Sept. 1995, 11.
18. Wang, Q.; Cao, J. Z.; Huang, J. G.; Xu, X. *Polym Eng Sci* 1997, 37, 1091.
19. Wang, Q.; Cao, J. Z.; Huang, J. G.; Xu, X. *Polym Int* 1996, 41, 245.
20. Peterlin, A. *Colloid Polym Sci* 1975, 253, 809.
21. Peterlin, A. *Polym Eng Sci* 1969, 9, 172.
22. Peterlin, A. *J Mater Sci* 1971, 6, 470.
23. Juska, T.; Harrison, I. K. *Polym Eng Rev* 1982, 2, 13.
24. Juska, T.; Harrison, I. K. *Polym Eng Sci* 1982, 22, 766.
25. Huang, H. *Studies on Structure Development and Changes in Properties of High Density Polyethylene and High Density Polyethylene/Calcium Carbonate Blends During Pan-Milling*, Ph.D. Thesis, Sichuan University, China, 1997.